Vibration analysis of line-coupled structures using a coupling load decomposition technique

M. Hatam, L. Cheng, and D. Rancourt
Mechanical Engineering Department, Laval University, Quebec G1K 7P4, Canada

(Received 4 February 1997; revised 28 October 1997; accepted 5 February 1998)

A new substructuring technique is proposed to perform vibration analysis of line-coupled structures. In dividing the whole structure into a master structure and several auxiliary structures, a variational formulation is used to model the master structure, enabling one to introduce the effects of all auxiliary structures by using their compliance characteristics at several observation points along the junction. Continuous functions of the compliance are obtained via a regression analysis. Given the problem of using the compliance inverse to attain a straightforward formulation, a ''Coupling Load Decomposition'' technique is proposed since a direct formulation using the compliance inverse is not feasible. By decomposing the interactive load between substructures, relations with displacement decomposition of the master structure can be found. This new formulation permits the direct use of the compliance of the junction, which may be obtained analytically, numerically, or experimentally. Numerical examples using both calculated and experimentally measured compliance data are given. Simulation results are also compared to those obtained experimentally, showing good agreement in low- and medium-frequency ranges. © *1998 Acoustical Society of America.* [S0001-4966(98)04205-2]

PACS numbers: 43.40.Dx, 43.40.At [CBB]

INTRODUCTION

Mechanical systems may be composed of different elements coupled together through points, lines, or surfaces. The complexity of such systems requires efficient simulation techniques. Moreover, some elements may be already complex so that any attempt to model all elements in the same manner becomes too demanding for most of the existing simulation techniques. From this point of view, the development of hybrid approaches that can make use of different simulation techniques becomes extremely attractive. Such a hybrid approach is proposed in this paper. The method is illustrated by analyzing the forced vibration of a plate coupled to different structures along continuous lines. Plate assemblies and stiffened plates are typical applications of such systems.

A number of techniques have been developed over the past few decades to study complex systems involving coupled structures. A good summary of the techniques is given by Min.[1] As far as planar structures are concerned, apart from some well-known techniques like the finite element methods, the statistical energy analysis method,[2] and the mobility power flow approaches,[3,4] many other investigations have been conducted to analyze particular configurations composed of coupled structures through continuous lines. Shen and Gibbs[5] have proposed a deterministic solution to study different configurations of rectangular plates at low frequencies. Guyader *et al.*[6] have used a technique based on analytical calculations of the eigenmodes of connected rectangular plates. The approach has been applied to platelike structures with a single junction. Other techniques have also been presented for platelike structures.[7,8] A semianalytical approach was also proposed using artificial springs to characterize the junction between substructures.[9] However, the technique becomes cumbersome when the number of substructures increases, since all substructures must be modeled with the same technique. Beam-stiffened plates is another category of coupled structures which has been investigated by some authors.[10,11] In an effort to develop a more general approach, Jezequel and Seito[12] have presented an extension of the classical component modal synthesis technique. The modal synthesis methods were reformulated to make them compatible with the finite element method.

In a real-life coupled system, there may exist some substructures with complex effects that can hardly be theoretically modeled. In such cases, experimental data are necessary to represent such substructures. However, very few methods allow structures identified by tests to be coupled through continuous interfaces. Some substructural or modal synthesis techniques are potentially capable of achieving the same task.[12–14] However, modal identification of complex structures may be a very difficult task, since it requires a detailed description of each substructure. Even if one is capable of obtaining the modal characteristics, they may be difficult to work with computationally.[15] On the contrary, compliance (or impedance, mobility) functions which carry the dynamic information of substructures are much easier to work with since measurements can only be conducted along the junction with other structures. Although some impedance or mobility model found in the literature[7,8] would be eventually modified to fit the hybrid requirement, methods should still be developed to incorporate measured data with the simulation model since they depend very much on the way in which the measured data are used in the whole formulation.

In this paper, a method using a regression approach to model the compliance distribution along continuous lines is presented. Complex systems are divided into a main structure and auxiliary structures. The main structure is analyzed using a variational formulation while the effects of all sub-

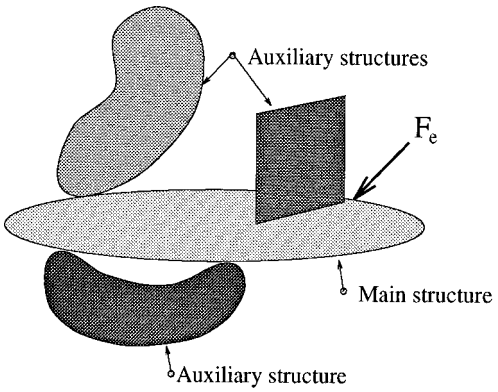

FIG. 1. A typical complex system.

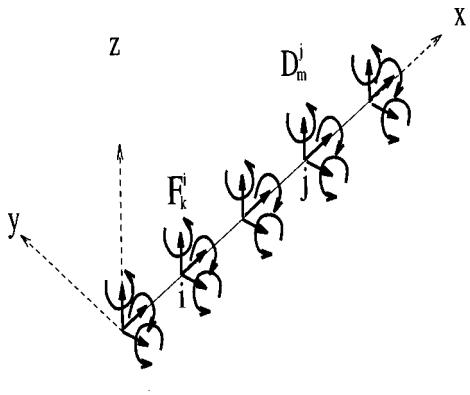

FIG. 2. Distribution of forces and moments due to coupling along a line.

structures are introduced using their compliances at the contact line with the main structure. Using a plate as the master structure, it is first demonstrated that direct use of compliance inverse data, which could have led to a straightforward formulation, results in an unstable solution. To address this problem, a new technique, named the ''Coupling Load Decomposition'' technique (CLD) is proposed. By decomposing the coupling load between substructures into a polynomial series, relations with the displacement of the master structure are found. Based on this new formulation, compliance data can be directly used with the help of a regression analysis.

Several examples are treated to numerically and experimentally assess the technique. A real-life structure demanding both numerical and experimental treatments is also presented to illustrate the hybrid aspect of the method. Whenever possible, simulated results are compared either to finite element simulations or to experimental data. The results are restricted to low- and middle-frequency ranges, since a semianalytical formulation is used to model the main structure. However, the proposed methodology is quite general and may be used in conjunction with any other energy-based formulations.

I. METHODOLOGY AND COUPLING REPRESENTATION

Consider a structure composed of different elements connected along continuous lines, or as a special case, through specific points. The whole structure is divided into two parts: a master structure and several auxiliary structures as shown in Fig. 1. The dynamic behavior of the master structure may be formulated using any energy-based approach which involves the effects of the auxiliary structures via their energy terms. In this paper, the formulation is based on a semianalytical approach using artificial springs inspired by our previous work.[9] The effects of all auxiliary structures are represented by their compliance characteristics. At each contact zone, compliance data may be obtained by treating each auxiliary substructure separately via any available approach: analytical, numerical, or experimental. Interfaces should then be developed to incorporate the effects of auxiliary structures.

In the case of a multipoint contact between two structures, the compliance $\beta^{ij}_{k'm'}$ is defined by the following relation

$$\beta^{ij}_{k'm'}=\frac{D^j_{k'}}{F^i_{m'}}, \tag{1}$$

where $D^j_{k'}$ is the displacement at point ''j'' in direction ''k''' due to a load $F^i_{m'}$, applied at point ''i'' in direction ''m'.'' If more than one contact point is involved, a compliance matrix should be used. When the contact zone between two coupled structures has dimensions comparable to the wavelength of the vibrating system, the point coupling representation is no more valid. In this case, each component of the compliance matrix is a continuous function of the excitation and response point coordinates.

The compliance variation along the junction may be obtained by first considering the line of contact as a combination of a finite number of contact points as shown in Fig. 2. A regression analysis leads to continuous functions representing the compliance components and ensures a continuous variation along the junction. Each component of the compliance matrix $\beta^{ij}_{k'm'}$ is replaced by a continuous function $\beta_{k'm'}(x,\xi)$. Here x and ξ indicate the local coordinate of the excitation and response points, respectively, along the contact line.

Consider a system composed of a thin rectangular plate as the master structure shown in Fig. 3, with $-b\leqslant x\leqslant b$,

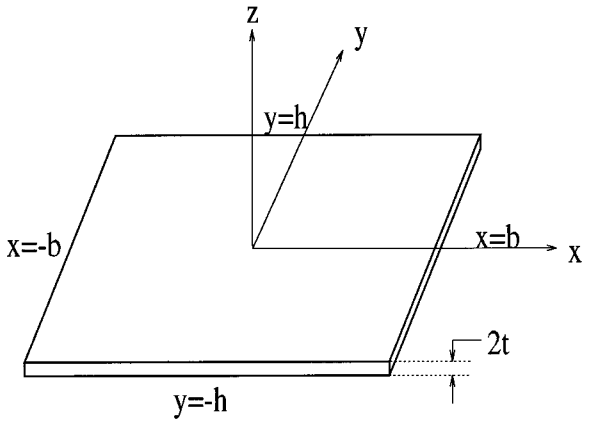

FIG. 3. A thin plate used as the main structure.

$-h \leqslant y \leqslant h$, and $-t \leqslant z \leqslant t$. The boundary conditions of the plate are modeled using artificial springs. Both translational and rotational springs are supposed to be uniformly distributed at each edge. Use of artificial springs enables one to simulate various boundary conditions. In the present work, small deformations are assumed and classical linear thin plate theory (Love–Kirchhoff) is used.

In order to achieve a general solution of the plate with arbitrary boundary conditions, an approximative solution can be obtained using the Rayleigh–Ritz method. The transverse displacement of the rectangular plate is approximated by a series:

$$w(x,y,t)=\sum_{i}^{\infty}\sum_{j}^{\infty} a_{ij} f_i(x) g_j(y), \tag{2}$$

where functions $f_i(x)$ and $g_j(y)$ are linearly independent. Assuming polynomial functions for $f_i(x)$ and $g_j(y)$ yields

$$w(x,y,t)=\sum_{i=0}^{m}\sum_{j=0}^{n} a_{ij}\left(\frac{x}{b}\right)^i\left(\frac{y}{h}\right)^j, \tag{3}$$

where the series is truncated to m and n terms, in the x and y directions, respectively. Appropriate values of m and n depend on the configuration of the plate and the desired frequency range.

Using the Rayleigh–Ritz method, the coefficients of the polynomial decomposition a_{ij} may be obtained by minimizing Lagrangian of the system L:

$$\frac{d}{dt}\left(\frac{\partial L}{\partial \dot{a}_{pq}}\right)-\left(\frac{\partial L}{\partial a_{pq}}\right)=0, \tag{4}$$

$$L=E_c-E_p^T+W, \tag{5}$$

with E_c and E_p^T being, respectively, the kinetic and total potential energies of the system. The term W represents the contribution of (or the work done by) surface loads or body forces. The total potential energy can be written as

$$E_p^T=E_p+E_p^b+E_p^{cp}, \tag{6}$$

where E_p is the total strain energy of the main structure, E_p^b is the potential energy stored at the boundary springs, and E_p^{cp} is the substructure contribution to the total energy of the coupled system. The energy approach and a double series of admissible functions for the field variable leads to the following forms of the energy terms

$$E_c=\frac{1}{2}\sum_{p}\sum_{q}\sum_{r}\sum_{s} M_{pqrs}\dot{a}_{pq}(t)\dot{a}_{rs}(t), \tag{7}$$

$$E_p+E_p^b+E_p^{cp}=\frac{1}{2}\sum_{p}\sum_{q}\sum_{r}\sum_{s} K_{pqrs}a_{pq}(t)a_{rs}(t), \tag{8}$$

where M_{pqrs} and K_{pqrs} are the general mass and stiffness of the system, respectively. The procedure for deriving the generalized mass and stiffness matrices of the plate (i.e., the main structure) with boundary springs and generalized force are explained in Ref. 16. It should be noted that the effect of the auxiliary structures are modeled through the term E_p^{cp}, which should be further analyzed.

II. CHARACTERIZATION OF AUXILIARY SUBSTRUCTURES

A. Direct formulation using compliance inverse matrix

Using the compliance inverse leads to a quite straightforward formulation. Assuming a junction parallel to the x axis, the coupling load vector between the main plate and an arbitrary substructure may be written as

$$F_{m'}(x)=\int_{-b}^{b}\sum_{k'}^{N} \eta_{k'm'}(x,\xi)D_{k'}(\xi)d\xi, \tag{9}$$

where $F_{m'}(x)$ and $D_{m'}(\xi)$ denote the functions representing the coupling load and the corresponding deformation variations, respectively, along the junction. It should be mentioned that the so-called ''coupling load'' represents the interacting effects between the connected substructures, which may be in the form of forces or moments. Consequently the corresponding deformations are translation and rotation, respectively. In the above equation, $\eta_{k'm'}(x,\xi)$ is the inverse of the compliance matrix of a substructure. Each component is a continuous function of x and ξ. The terms ''k''' and ''m''' vary from 1 to N and N denotes the number of coupling load components along the junction and depends on the configuration. In a general problem where all degrees of freedom are present, N is equal to 6. The energy term stored in the substructure, in its general form, can be written as

$$E_{cp}=\frac{1}{2}\int_{-b}^{b}\sum_{m'}^{N} F_{m'}(x)D_{m'}(x)dx. \tag{10}$$

Applying Eq. (9) yields

$$E_{cp}=\frac{1}{2}\int_{-b}^{b}\int_{-b}^{b}\sum_{k'}^{N}\sum_{m'}^{N} \eta_{k'm'}(x,\xi)D_{k'}(\xi)D_{m'}(x)d\xi\, dx. \tag{11}$$

In order to derive the compliance matrix, the junction line is discretized into a series of observation points as illustrated in Fig. 2. By applying a unit excitation at point i while measuring the response at point j, the compliance matrix $\beta_{ij}^{k'm'}$ can be constructed. The inverse of this matrix gives $\eta_{ij}^{k'm'}$. A polynomial regression analysis can then be performed on η, and a continuous function $\eta_{k'm'}(x,\xi)$ can be found as follows:

$$\eta_{k'm'}(x,\xi)=\sum_{k=0}^{n1}\sum_{l=0}^{n2} c_{kl}^{k'm'}x^k\xi^l, \tag{12}$$

where $c_{kl}^{k'm'}$ denotes the regression coefficients and ''$n1$'' and ''$n2$'' are the degree of regression for independent variables x and ξ, respectively. The regression technique is briefly explained in the Appendix. Notice that the procedure is, in principle, applicable to the analysis of both the compliance and its inverse. For special cases when there is only one compliance function $F_{m'}(x)$ at the junction or in any special case where the substructure compliance inverse $\eta_{m'm'}(x,\xi)$ is decoupled from other components, the energy contribution

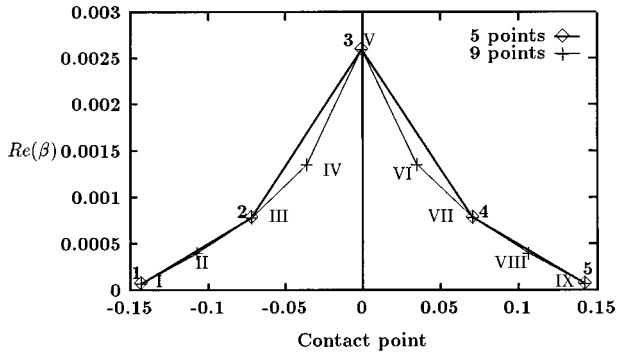

FIG. 4. Variation of the real part of β along the line of contact.

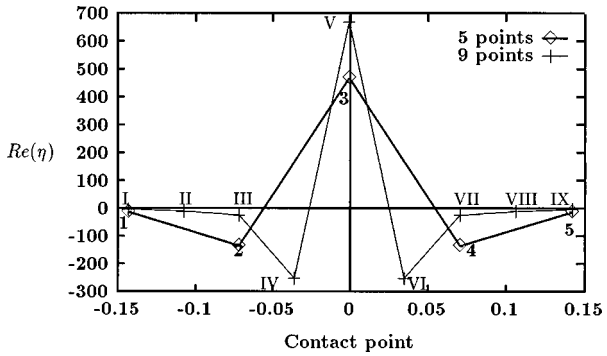

FIG. 5. Variation of the real part of η along the line of contact.

of the substructure, given by Eq. (11), can be written as

$$E_{cp}=\frac{1}{2}\int_{-b}^{b}\int_{-b}^{b}\eta_{m'm'}(x,\xi)D_{m'}(\xi)D_{m'}(x)d\xi\,dx. \quad (13)$$

This equation may then be used to obtain the generalized stiffness matrix representing the contribution of substructures on the vibration of the coupled system. As we can notice, this formulation is quite straightforward and is based, however, on a successful regression analysis on the η matrix. This issue is addressed below.

The formulation developed previously uses the compliance inverse function (or matrix) η. The direct measurement of this quantity is not feasible, since there is no practical way of introducing a unit displacement at one location, while keeping the other locations fixed. On the contrary, the compliance matrix β is much easier to obtain. In this case, the compliance matrix must be inverted to obtain the η matrix. However, this inversion process becomes difficult when the number of contact points is increased. This phenomenon has been explained by Fung[17] for the flexibility matrix which is a special case of the compliance matrix in the static case. It turns out that when the number of observation points approaches infinity, the distance between adjacent points approaches zero and the components of the η matrix approach infinity. As a result, by increasing the number of contact points, the compliance matrix becomes hardly invertible.

Apart from the problem mentioned above, inherent to the characteristics of the η function, an additional problem emerges when a regression analysis should be further performed on the η matrix. To illustrate this problem, let us consider how the compliance function β and the compliance inverse function η vary with the number of observation points. A simply supported rectangular thin plate (Fig. 3) is taken as an example, whose rotational compliance β_{44}^{ij} and its inverse along one edge ($y=-h$) are studied. The plate used is made of aluminum with dimensions $b=15$ cm, $h=22.5$ cm, and $t=15.875$ mm. Figure 4 shows the variation of the β matrix when a unit torque is applied at the midpoint of the junction ($x=0$) and the rotational responses are measured at different contact points along the junction. Two curves using, respectively, five and nine contact points are presented. In the case of nine observation points, points I, III, V, VII, and IX have the same coordinates as points 1, 2, 3, 4, and 5, in the five observation point case. Points II, IV, VI, and VIII are four new observation points added to form the nine contact points case. It can be observed, in Fig. 4, that in both cases, the compliance values are the same for each common observation point. Obviously, the nine point configuration defines the compliance characteristics of the plate more precisely than the five point configuration does. The smoothness of the compliance variation makes it possible to perform a stable regression analysis.

Under the same conditions, Fig. 5 shows the variation of η. Again, two curves denote the η variations for the five and nine contact point cases, respectively. It can be seen that the value of η at an arbitrary point strongly depends on the number of contact points. For example, although points 2, 3, and 4 have the same coordinates as points III, V, and VII, values of η considerably vary from one case to another for these common points. This strong dependency on the number of contact points is such that the regression analysis on the η matrix should be avoided. Therefore a new formulation is required to directly use the compliance matrix.

B. Formulation via coupling load decomposition

A new formulation is proposed to avoid the use of the η matrix in the computation of the energy contributed by the substructures. A load distribution along the junction is considered and efforts are made to find a relation between the coefficients of the load distribution and coefficients of previously defined displacement fields. The formulation is developed for an arbitrary load distribution which can either be forces or moments. At this point, for the sake of briefness, it is supposed that there is no coupling between coupling loads of different natures (forces and moments corresponding to a different degree of freedom, for example) and, accordingly, the summation term in Eq. (9) can be removed. It should be noted that in cases where this simplification does not apply, the formalism that will be developed still remains valid, although the mathematical description will be different. Equation (9) can be rewritten in the following form to relate the displacement of the junction $D_{m'}(x)$ to the load function $F_{m'}(x)$ using the compliance function $\beta_{m'm'}(x,\xi)$

$$D_{m'}(x,y_0)=\int_{-b}^{b}\beta_{m'm'}(x,\xi,y_0)F_{m'}(\xi,y_0)d\xi. \quad (14)$$

In the above expression, the junction is obviously assumed to be parallel to the x axis with y_0 as its y coordinate. A regression analysis over the compliance matrix gives

$$\beta_{m'm'}(x,\xi,y_0)=\sum_{k=0}^{n1}\sum_{l=0}^{n2} c_{kl}^{m'm'}x^k\xi^l. \tag{15}$$

Inserting Eq. (15) into Eq. (14) yields

$$D_{m'}(x,y_0)=\int_{-b}^{b}\sum_{k=0}^{n1}\sum_{l=0}^{n2} c_{kl}^{m'm'}x^k\xi^l F_{m'}(\xi,y_0)d\xi. \tag{16}$$

In the above expression, the load distribution $F_{m'}(\xi,y_0)$ is an unknown function which constitutes the major obstacle when using the compliance matrix. To tackle this problem, the load distribution along the junction is decomposed over a polynomial base as

$$F_{m'}(\xi,y_0)=\sum_{i}^{m}\sum_{j}^{n} b_{ij}\left(\frac{\xi}{b}\right)^i\left(\frac{y_0}{h}\right)^j, \tag{17}$$

with b_{ij} being unknown coefficients to be determined. Hence Eq. (16) may be written as

$$D_{m'}(x,y_0)=\int_{-b}^{b}\sum_{k=0}^{n1}\sum_{l=0}^{n2}\sum_{i}^{m}\sum_{j}^{n} c_{kl}^{m'm'}b_{ij}x^k\xi^l \times\left(\frac{\xi}{b}\right)^i\left(\frac{y_0}{h}\right)^j d\xi. \tag{18}$$

The polynomial decomposition for transverse displacements of a rectangular thin plate given by Eq. (3) may be written in a more general form for $D_{m'}(x,y)$ as

$$D_{m'}(x,y)=\sum_{i=0}^{m}\sum_{j=0}^{n} B_{ij}\left(\frac{x}{b}\right)^i\left(\frac{y}{h}\right)^j. \tag{19}$$

Inserting this polynomial decomposition in Eq. (18) yields

$$\sum_{i}^{m}\sum_{j}^{n} B_{ij}\left(\frac{x}{b}\right)^i\left(\frac{y_0}{h}\right)^j=\int_{-b}^{b}\sum_{k=0}^{n1}\sum_{l=0}^{n2}\sum_{i}^{m}\sum_{j}^{n} c_{kl}^{m'm'}b_{ij}x^k\xi^l \times\left(\frac{\xi}{b}\right)^i\left(\frac{y_0}{h}\right)^j d\xi. \tag{20}$$

After integrating with respect to ξ, the following relation is obtained

$$\sum_{i}^{m}\sum_{j}^{n} B_{ij}\left(\frac{x}{b}\right)^i\left(\frac{y_0}{h}\right)^j =\sum_{k=0}^{n1}\sum_{l=0}^{n2}\sum_{i}^{m}\sum_{j}^{n} c_{kl}^{m'm'}b_{ij} \times\left(\frac{y_0}{h}\right)^j\frac{b^{l+1}}{i+l+1}(1+(-1)^{i+l})x^k. \tag{21}$$

In order to find the relation between two series of coefficients B_{ij} and b_{ij}, the two sides of the above equation are multiplied by x^τ, where $\tau=0,...,m$. Integrating the resulting equation with respect to x along the junction yields

$$\sum_{i}^{m}\sum_{j}^{n} B_{ij}\frac{b^{\tau+1}}{i+\tau+1}\left(\frac{y_0}{h}\right)^j(1+(-1)^{\tau+i}) =\sum_{i}^{m}\sum_{j}^{n}\sum_{k=0}^{n1}\sum_{l=0}^{n2} c_{kl}^{m'm'}b_{ij}\left(\frac{y_0}{h}\right)^j \times\frac{b^{k+l+\tau+2}}{(i+l+1)(k+\tau+1)} \times(1+(-1)^{i+l})(1+(-1)^{k+\tau}). \tag{22}$$

Two series of coefficients are defined as

$$\Gamma_i=\sum_{j} b_{ij}\left(\frac{y_0}{h}\right)^j, \tag{23}$$

$$\Omega_i=\sum_{j} b_{ij}\left(\frac{y_0}{h}\right)^j. \tag{24}$$

The above procedure is only valid at the junction, and accordingly, a complete relation between the series of coefficients B_{ij} and b_{ij} is not available. Fortunately, only the global relation between two series of new coefficients Γ_i and Ω_i is needed in the formulation. This relation can be found by inserting Eqs. (23) and (24) in Eq. (22) as

$$\sum_{i}^{m}\Gamma_i\frac{b^{\tau+1}}{i+\tau+1}(1+(-1)^{\tau+i}) =\sum_{i}^{m}\sum_{k=0}^{n1}\sum_{l=0}^{n2} c_{kl}^{m'm'}\Omega_i\frac{b^{k+l+\tau+2}}{(i+l+1)(k+\tau+1)} \times(1+(-1)^{i+l})(1+(-1)^{k+\tau}). \tag{25}$$

Note that the above equation is valid for each value of $\tau=0,...,m$ so that the whole set of equations can be written in matrix form as

$$\underset{(\hat{m}\times\hat{m})(\hat{m}\times 1)}{[\Delta]}\ \{\Gamma\}=\underset{(\hat{m}\times\hat{m})(\hat{m}\times 1)}{[\Lambda]}\ \{\Omega\}, \tag{26}$$

where $\hat{m}=m+1$,

$$\Delta(i,j)=\frac{b^{i+1}}{i+j+1}(1+(-1)^{i+j}) \tag{27}$$

and

$$\Lambda(i,j)=\sum_{k=0}^{n1}\sum_{l=0}^{n2} c_{kl}^{m'm'}\frac{b^{k+l+i+2}}{(i+l+1)(k+i+1)} \times(1+(-1)^{i+k})(1+(-1)^{j+l}). \tag{28}$$

Consequently,

$$\underset{(\hat{m}\times 1)}{\{\Omega\}}=\underset{(\hat{m}\times\hat{m})}{[\Lambda]^{-1}}\ \underset{(\hat{m}\times\hat{m})(\hat{m}\times 1)}{[\Delta]}\ \{\Gamma\}. \tag{29}$$

Finally, the following relation between the two series of coefficients Γ_i and Ω_i is obtained

$$\{\Omega\}=[H]\{\Gamma\} \tag{30}$$

where

$$[H]=[\Lambda]^{-1}[\Delta]. \tag{31}$$

The substructural energy term, resulting from the presence of the coupling load $F_{m'}(\xi,y_0)$ on the main plate, is then calculated as

$$E_{cp}=\frac{1}{2}\int_{-b}^{b}F_{m'}(x,y_0)D_{m'}(x,y_0)dx$$

$$=\frac{1}{2}\int_{-b}^{b}\sum_i\sum_j\sum_r B_{ij}\Omega_r\left(\frac{y_0}{h}\right)^j\left(\frac{x}{b}\right)^{i+r}, \tag{32}$$

where

$$F_{m'}(x,y_0)=\sum_r \Omega_r\left(\frac{x}{b}\right)^r, \tag{33}$$

$$\Omega_r=\sum_j b_{rj}\left(\frac{y_0}{h}\right)^j. \tag{34}$$

After integrating along the junction, Eq. (32) becomes

$$E_{cp}=\frac{1}{2}\sum_i\sum_j\sum_r B_{ij}\Omega_r\left(\frac{y_0}{h}\right)^j$$

$$\times\frac{b}{(i+r+1)}\,(1+(-1)^{i+r}). \tag{35}$$

One may write Eq. (30) in the following form

$$\Omega_r=\sum_s H_{rs}\Gamma_s. \tag{36}$$

Hence Eq. (35) is given as

$$E_{cp}=\frac{1}{2}\sum_i\sum_j\sum_r\sum_s B_{ij}\Gamma_s H_{rs}\left(\frac{y_0}{h}\right)^j$$

$$\times\frac{b}{(i+r+1)}\,(1+(-1)^{i+r}), \tag{37}$$

where

$$\Gamma_s=\sum_t B_{st}\left(\frac{y_0}{h}\right)^t. \tag{38}$$

The final form of the substructure energy is obtained by replacing the above equation in Eq. (37)

$$E_{cp}=\frac{1}{2h^2}\sum_i\sum_j\sum_p\sum_q\sum_r jqB_{ij}B_{pq}H_{rp}\left(\frac{y_0}{h}\right)^{q+j-2}$$

$$\times\frac{b}{(i+r+1)}\,(1+(-1)^{i+r}), \tag{39}$$

where $i,p,r=0,...,m$ and $j,q=0,...,n$. Differentiation must be conducted to obtain the substructural stiffness matrix

$$\frac{\partial E_{cp}}{\partial B_{ij}}=\frac{1}{2}\sum_p\sum_q\sum_k B_{pq}b\left(\frac{y_0}{h}\right)^{q+j}$$

$$\times\left\{\frac{H_{kp}}{(i+k+1)}\,(1+(-1)^{i+k})+\frac{H_{ki}}{(p+k+1)}\right.$$

$$\left.\times(1+(-1)^{p+k})\right\}. \tag{40}$$

Finally, the generalized stiffness matrix due to the mth component of the coupling loads is obtained.

$$k_{pqrs}^{cp}=\frac{1}{2}\sum_k b\left(\frac{y_0}{h}\right)^{q+s}\left\{\frac{H_{kp}}{(r+k+1)}\,(1+(-1)^{r+k})\right.$$

$$\left.+\frac{H_{kr}}{(p+k+1)}\,(1+(-1)^{p+k})\right\}. \tag{41}$$

It is a complex frequency-dependent matrix which must be added to the previously developed stiffness matrices of the main structure.

Several factors affect the accuracy of the present formulation. Limiting the infinite series in Eq. (2) to a finite series is a computational restriction. The general criteria for truncating the series is to ensure sufficient accuracy in the resulting solutions. The number of terms in the series is therefore increased until no significant variations are noticed in the frequency range of interest. This problem, related to the Rayleigh–Ritz method, has been fully discussed.[9]

The determination of the degree of the polynomial series in the regression analysis is also an important factor. In general, the maximum degree of the polynomial should be chosen in such a way that the number of coefficients does not exceed the number of samples so that

$$(n1+1)\times(n2+1)\leqslant(np)^2, \tag{42}$$

where ''$n1$'' and ''$n2$'' are the degree of regression for independent variables x and ξ, respectively, and np is the number of observation points. The proposed regression technique permits minimizing errors when more contact points are used.

The choice of the appropriate number of observation points plays an important role in determining the accuracy of this hybrid approach. During our simulations, it was noted that the discretization distance should be at least four or five times smaller than the minimum wavelength in the frequency range of interest. This ensured an acceptable representation of the compliance variation along the junction. The same criteria is used in finite element analysis to estimate a sufficient number of elements for modal analysis of structures.

III. NUMERICAL APPLICATIONS

The developed technique has been applied to a series of platelike structures and beam-stiffened plates. In the forthcoming examples, the components of the coupled system are made of aluminum with modulus of elasticity $E=0.7E+11$ N/m^2, mass density $\rho=2700$ kg/m^3, and Poisson's ratio $\nu=0.3$. A damping factor $\xi=0.01$ is used in all cases. The main plate is 30-cm wide ($2b$), 45-cm long ($2h$) and 3.175-mm thick ($2t$). In all cases, nine observation points are considered with $n1=n2=8$, where ''$n1$'' and ''$n2$'' are the degree of regression for the two independent variables, respectively.

The first example considers two plates connected together along one edge to form an L-shaped plate. Both plates are simply supported along their edges and, consequently, only a rotational moment distribution along the junction is

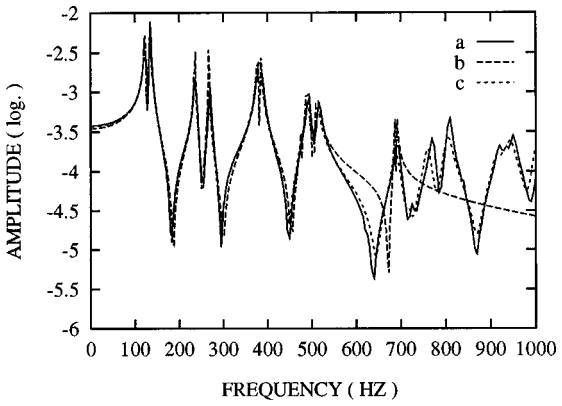

FIG. 6. Response of an L-shaped plate, (a) CLD technique, (b) FE method using the first 12 modes, (c) FE method using the first 24 modes.

present. A transverse force excitation of 100 N is applied at point $x=y=7.5$ cm of the main plate and the transversal response is calculated at the same point.

A finite element simulation using the IDEAS package is conducted to validate the CLD technique. Linear quadrilateral thin shell elements have been used and mode superposition is applied to derive the response of the coupled system up to 1000 Hz. Figure 6 shows the comparison between the two methods. The response of the coupled system is shown when 12 or 24 modes of vibration are superimposed. Good agreement is observed between the CLD technique and the finite element method using 24 modes over the frequency band of interest.

Another example is presented in Fig. 7 using a ribbed plate. The previously used plate is stiffened by three identical stiffeners with cross section 1.5×0.9 cm along lines $y=0.125$ m, $y=0$ m, and $Y=-0.125$ m. The presence of the stiffeners introduces two kinds of coupling with the plate. The first one is related to the torsional effect of the beam which includes a distribution of torsional moment along the junction, and the second one is due to its flexural stiffness, which includes a transverse force distribution. Assuming small deformations,the torsional and flexural behavior of the beam are decoupled and may be treated separately to form two generalized stiffness matrices related to the torsional and transverse vibrations of the stiffener. The compliances were derived semianalytically in this case. Again, comparisons

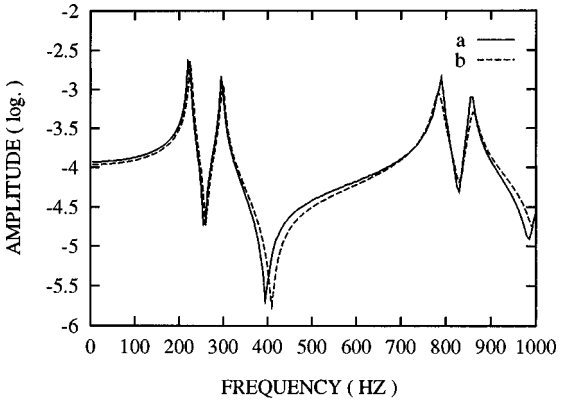

FIG. 7. Responses of the plate stiffened by three identical beams: (a) CLD technique, (b) finite element model.

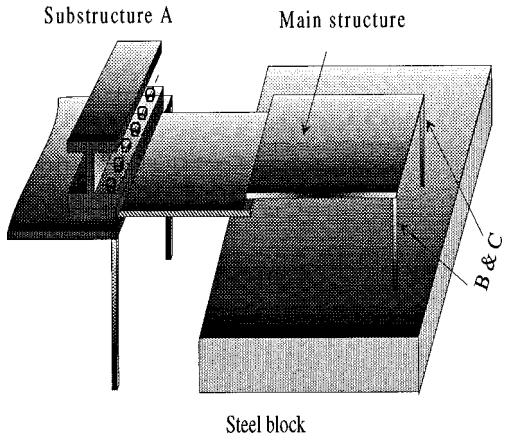

FIG. 8. Schematic view of the complex structure under study.

with FE simulation validates the CLD technique.

The advantage of the proposed technique in dealing with structures with identical elements is quite obvious. The generalized stiffness matrix of a substructure may be obtained as a function of the global coordinates of the connection line. When the number of contact points and the degree of regression for different substructures remain unchanged, the dynamic stiffness matrix related to a series of identical substructures can be simply obtained. A typical indication of the computation efficiency of the approach can be shown using a previously treated L-shaped plate by increasing the number of auxiliary plates. It was shown that there is typically an increase of 140% in processing time when six other plates are added to the original configuration.

IV. EXPERIMENTAL APPLICATIONS

As an example to show the hybrid aspect of the method, a system composed of simple and complex elements is investigated. Figure 8 shows a schematic view of the system that was studied. The whole structure consists of a thin steel plate (45.7-cm long, 30.5-cm wide, and 2.3-mm thick) as the main structure. The coordinate system is located at the center of the plate. Two steel circular rods with a radius of 3.2 mm and a length of 15.6 cm were coupled to the plate at the two corners. The main structure was supported by a more complex substructure along the line $y=-22.9$ cm. This support substructure was composed of a plate (30.5-cm wide, 45.7-cm long, 5.1-mm thick) which is connected to a steel table. Notice that the supporting plate has similar dimensions and properties to the main plate to ensure an effective coupling between both. The main plate is held by the supporting plate and caught between two symmetrical notches. The bolts were tightened so that both the main structure and the supporting plate underwent the same translational movement along the line of junction. At the same time, no moment was transmitted across the plates.

Different procedures were used to get the compliance characteristics of the subsystems. For each of the steel rods (substructures B and C), the translational compliance in the axial direction of the rod, as well as two bending compliance terms were calculated using a classical approach. Since only the flexural vibration of the main structure is considered,

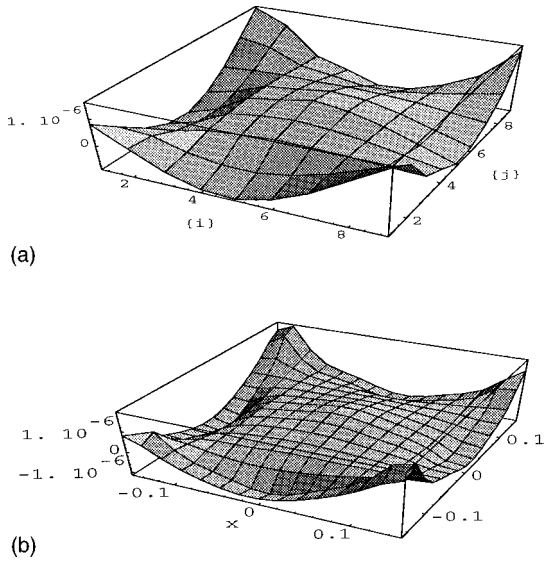

FIG. 9. Variation of the real part of the compliance function of substructure A at a frequency of 420 H. (a) Measured values, (b) result of the regression analysis.

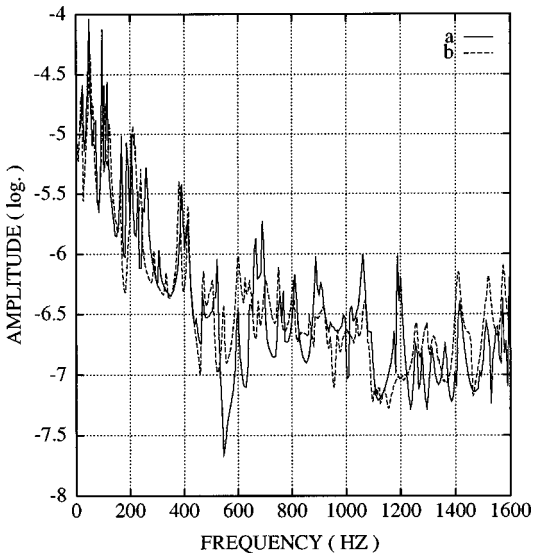

FIG. 10. Frequency response function of the complex structure. (a) Hybrid method and (b) experimental measurements.

other components of interactive forces and moments related to the in-plane vibration of the main structure were neglected. Substructure A (supporting plate with the steel table) is, by itself, a complex system composed of different elements. Experimental measurements were conducted at nine observation points along the line of contact to obtain the compliance matrix. A regression analysis was then performed on the measured data. At each observation point along the contact line, the supporting plate was excited by a shaker driven by a broadband random signal produced by an analyzer. Transverse responses were measured at all observation points using an accelerometer. The two measured signals, the acceleration and the force, were then captured by the analyzer to compute the compliance function. In order to enhance the quality of the measurements, a mass correction procedure was used to compensate for the effect of the added mass due to the exciter and the force transducer.[19]

Figure 9 shows the variation of the real component of the compliance function of the supporting structure at 420 Hz. Both measured data and the results of the regression analysis with $n1=n2=7$ are compared. In this figure, ''i'' denotes the excitation point and ''j,'' the response point. It can be seen that the regression model adequately represents the compliance variation as a continuous function.

Using these compliance data, the response of the whole system is calculated using the hybrid approach. Experimental measurements were also carried out to validate the simulation results. In both cases, the excitation is a unit transverse harmonic force applied at point (8.35, 7.0). The displacement response of the structure was obtained using an average over three points (12.25, 3.0), $(-12.25, 3.0)$, and (3.25, 14.3), with all coordinates in centimeters.

Simulated results and experimental data are compared up to 1600 Hz in Fig. 10. Generally speaking, results suggest that the hybrid model works reasonably well to predict the general trend of the structure in the whole frequency range of interest. Considering the fact that a large number of structural modes are involved, one gets a good appreciation of the hybrid method's ability to handle complex structures. Agreement between the two sets of results is excellent up to about 600 Hz, where 16 modes of vibration are involved. The deviation at higher frequencies indicates that there is still room for improvement in both experimental and numerical aspects. One of the plausible factors may be the fact that the condition of line coupling (which is supposed to transmit only transverse forces) becomes doubtful at higher frequencies. Also, the variational formulation with polynomial decomposition has been shown to be reliable mainly at low frequencies. The developed method permits the use of any other energy based formulations involving the effects of the auxiliary structures via their energy terms. As a result, alternative formulations on the main structure may improve the precision of the technique at higher frequencies.

V. CONCLUSIONS

Vibrations of coupled structures along a continuous line have been investigated. Difficulties inherent to the inversion of the β matrix and the feasibility of a regression analysis on the η matrix has been illustrated. It was shown that the value of η at a fixed point significantly varies with the number of contact points and, accordingly, the regression analysis does not converge toward a correct estimation of the η function. This point prevents the use of a direct formulation. To tackle the problem, a new approach, based on the direct use of the compliance matrix via a coupling load decomposition technique was proposed. The approach was illustrated for systems composed of a thin plate as the main structure. The approach is versatile enough to include both calculated and experimentally measured compliance data of the substructures. This hybrid feature may allow one to go beyond the limit of the most commonly used approaches to handle more complex structures. Vibrations of typical coupled structures along a continuous line were investigated. Numerical results were compared to finite element models and good agreement was observed. The proposed approach was also applied to a

real-life configuration which required different treatment for each substructure. Comparisons with experimental data showed good agreement in a frequency range involving a large number of structural modes.

Further improvement of the approach should focus on its extension to higher frequency applications. Extension of the method to cases where all possible degree of freedoms exist along the junction requires the development of reliable compliance measurement techniques (especially rotational terms).

APPENDIX: REGRESSION ANALYSIS ON THE COMPLIANCE MATRIX OR ITS INVERSE

The linear model for relating a dependent variable Y to p-independent variables is

$$Y_i = \alpha_0 + \alpha_1 x_{i1} + \alpha_2 x_{i2} + \cdots + \alpha_p x_{ip}, \tag{A1}$$

where subscript i, varying from one to n, indicates the observation unit from which data Y and p-independent variables are taken. The second subscript designates the independent variable. Hence there are $(p+1)$ coefficients α to be estimated. For convenience, let us assume that $p' = p+1$. In matrix form, one has

$$\mathbf{Y} = \mathbf{X}\alpha, \tag{A2}$$

where Y is a $n \times 1$ column vector observation on the dependent variables Y_i; X a $n \times p'$ matrix consisting of a column of ones, followed by the p column vectors of the observations on the independent variables; A least-squares estimate on the optimal values of coefficients α_i can be obtained by

$$\hat{\alpha} = (\mathbf{X^T X})^{-1}(\mathbf{X^T Y}), \tag{A3}$$

where $\mathbf{X^T}$ is the transpose of matrix $\mathbf{X}$.

The most frequently used curvilinear response model, in practice, is a polynomial regression model. As a special case of the general linear regression model,[18] it is easy to handle. This model can contain, one, two, or more independent variables. In the case where two variables are used, the $\mathbf{X}$ matrix can be written as

$$\mathbf{X} = \begin{bmatrix} 1 & X_{11} & X_{12} & X_{11}^2 & X_{12}^2 & X_{11}X_{12} & \cdots \\ 1 & X_{21} & X_{22} & X_{21}^2 & X_{22}^2 & X_{21}X_{22} & \cdots \\ \vdots & \vdots & \vdots & \vdots & \vdots & \vdots & \\ 1 & X_{n1} & X_{n2} & X_{n1}^2 & X_{n2}^2 & X_{n1}X_{n2} & \cdots \end{bmatrix}. \tag{A4}$$

This regression analysis technique may be applied to the compliance function β which is approximated by a polynomial of two variables. For example the rotational term β_{44}^{ij} can be defined as

$$\beta_{44}^{ij}(x,\xi) = \sum_{k=0}^{n1} \sum_{l=0}^{n2} c_{kl}^{44} x^k \xi^l. \tag{A5}$$

Using the above definition, Eq. (A2) may be written in the following form

$$\begin{Bmatrix} \beta_{44}^{11} \\ \beta_{44}^{12} \\ \vdots \\ \beta_{44}^{1z} \\ \beta_{44}^{21} \\ \beta_{44}^{22} \\ \vdots \\ \beta_{44}^{2z} \\ \vdots \\ \beta_{44}^{zz} \end{Bmatrix} = \begin{bmatrix} 1 & x_1^0\xi_1^1 & \cdots & x_1^0\xi_1^{n2} & x_1^1\xi_1^1 & \cdots & x_1^1\xi_1^{n2} & \cdots & x_1^{n1}\xi_1^{n2} \\ 1 & x_1^0\xi_2^1 & \cdots & x_1^0\xi_2^{n2} & x_1^1\xi_2^1 & \cdots & x_1^1\xi_2^{n2} & \cdots & x_1^{n1}\xi_2^{n2} \\ \vdots & \vdots & & \vdots & \vdots & & \vdots & & \vdots \\ 1 & x_1^0\xi_z^1 & \cdots & x_1^0\xi_z^{n2} & x_1^1\xi_z^1 & \cdots & x_1^1\xi_z^{n2} & \cdots & x_1^{n1}\xi_z^{n2} \\ 1 & x_2^0\xi_1^1 & \cdots & x_2^0\xi_1^{n2} & x_2^1\xi_1^1 & \cdots & x_2^1\xi_1^{n2} & \cdots & x_2^{n1}\xi_1^{n2} \\ 1 & x_2^0\xi_2^1 & \cdots & x_2^0\xi_2^{n2} & x_2^1\xi_2^1 & \cdots & x_2^1\xi_2^{n2} & \cdots & x_2^{n1}\xi_2^{n2} \\ \vdots & \vdots & & \vdots & \vdots & & \vdots & & \vdots \\ 1 & x_2^0\xi_z^1 & \cdots & x_2^0\xi_z^{n2} & x_2^1\xi_z^1 & \cdots & x_2^1\xi_z^{n2} & \cdots & x_2^{n1}\xi_z^{n2} \\ \vdots & \vdots & & \vdots & \vdots & & \vdots & & \vdots \\ 1 & x_z^0\xi_z^1 & \cdots & x_z^0\xi_z^{n2} & x_z^1\xi_z^1 & \cdots & x_z^1\xi_z^{n2} & \cdots & x_z^{n1}\xi_z^{n2} \end{bmatrix} \begin{Bmatrix} c_{0\ 0}^{44} \\ c_{0\ 1}^{44} \\ \vdots \\ c_{0\ n2}^{44} \\ c_{1\ 0}^{44} \\ c_{1\ 1}^{44} \\ \vdots \\ c_{1\ n2}^{44} \\ \vdots \\ c_{n1\ n2}^{44} \end{Bmatrix}, \tag{A6}$$

where $\mathbf{Y}$, a column vector $(n \times 1)$, is a vector representation of β as stated above. $z = 1,...,np$, $n = np \times np$ where np is the number of selected contact points or observation points. The $\mathbf{X}$ matrix is a $(n \times \hat{n})$ matrix where $\hat{n} = (n1+1) \times (n2+1)$ with $n1$ and $n2$ being the maximum degree of x and ξ in the response surface function, respectively. Hence the vector of parameters, consisting of the elements of c_{kl}^{44}, is a column vector with dimension $(\hat{n} \times 1)$. In a regression analysis, the number of observations must be equal or greater than the number of parameters.

The dependent variable vector $\mathbf{Y}$ is a frequency-dependent vector. It means that the above process must be repeated for each frequency. It seems to be a relatively tedious approach. Fortunately, as long as the observation points remain unchanged for different frequencies, the $\mathbf{X}$ matrix remains the same. Therefore at each frequency, parameters α are obtained by the following relation

$$\hat{\alpha}(\omega) = \overline{\mathbf{X}}\mathbf{Y}, \tag{A7}$$

where $\overline{X}$ can be calculated by

$$\overline{\mathbf{X}} = (\mathbf{X^T X})^{-1}\mathbf{X^T}. \tag{A8}$$

As explained before, matrix $\overline{\mathbf{X}}$ depends only on independent variables and, accordingly, does not change with frequency

if the number and location of observation points remain unchanged. It is clear that at higher frequencies, the shape of the compliance curve along the junction line becomes more complicated and more observation points are required. Matrix $\overline{\mathbf{X}}$ must be recalculated after each change in the number of contact points. This constitutes the major part of the regression analysis and takes more than 80% of the total required time for the analysis. Therefore it is recommended to choose a sufficient number of observation points for a relatively large band of frequency to avoid recalculation of $\overline{\mathbf{X}}$ too frequently.

The whole procedure gives an analytical expression for estimating the variation of the compliance between an excitation point ξ and the response point x in the form of $\beta(x,\xi)$ along the junction. It is written as

$$\beta(x,\xi)=\psi^{\mathbf{T}}\alpha, \tag{A9}$$

where

$$\psi^{\mathbf{T}}=[1 \quad x^0\xi^1 \quad \cdots \quad x^0\xi^{n2} \quad x^1\xi^1 \quad \cdots \quad x^1\xi^{n2} \quad \cdots \quad x^{n1}\xi^{n2}], \tag{A10}$$

$$\alpha=\{c_{0\,0} \quad c_{0\,1} \quad \cdots \quad c_{0\,n2} \quad c_{1\,0} \quad c_{1\,1} \quad \cdots \quad c_{1\,n2} \quad \cdots \quad c_{n1\,n2}\}. \tag{A11}$$

[1] K. W. Min, T. Igusa, and J. D. Achenbach, ''Frequency window method for forced vibration of structures with connected substructures,'' J. Acoust. Soc. Am. **92**, 2726–2733 (1992).

[2] R. H. Lyon, *Statistical Energy Analysis of Dynamical Systems, Theory and Applications* (MIT, Cambridge, MA, 1975).

[3] H. G. D. Goyder and R. G. White, ''Vibrational power flow from machines into built up structures, Part I: Introduction and approximate analysis of beam and plate-like foundations,'' J. Sound Vib. **68**, 59–75 (1980).

[4] R. J. Pinnington and R. G. White, ''Power flow through machine isolators to resonant and non-resonant beams,'' J. Sound Vib. **75**, 179–197 (1981).

[5] Y. Shen and B. M. Gibbs, ''An approximate solution for the bending vibration of a combination of rectangular thin plates,'' J. Sound Vib. **105**, 73–90 (1986).

[6] J. L. Guyader, C. Boisson, P. Millot, and C. Lesueur, ''Energy transmission in finite coupled plates, part I: Theory,'' J. Sound Vib. **81**, 81–92 (1982).

[7] J. M. Cushieri, ''Structural power-flow analysis using a mobility approach of an *L*-shaped plate,'' J. Acoust. Soc. Am. **87**, 1159–1165 (1990).

[8] B. Petersson, ''A thin-plate model for the moment mobility at the intersection of two perpendicular plates,'' J. Sound Vib. **108**, 471–485 (1986).

[9] L. Cheng and J. Nicolas, ''Free vibration analysis of a cylindrical shell-circular plate system with general coupling and various boundary conditions,'' J. Sound Vib. **155**, 231–247 (1992).

[10] E. Goldfracht and G. Rosenhouse, ''Use of Lagrange multipliers with polynomial series for dynamic analysis of constrained plates, Part I: Polynomial series,'' J. Sound Vib. **92**, 83–93 (1984).

[11] L. J. Hu, I. Smith, and Y. H. Chui, ''Vibration analysis of ribbed plates with a rigid intermediate line support,'' J. Sound. Vib. **178**, 163–175 (1994).

[12] L. Jezequel and H. D. Seito, ''Component modal synthesis methods based on hybrid models, Part I: Theory of hybrid models and modal truncation methods,'' Trans. ASME, J. Appl. Mech. **61**, 100–108 (1994).

[13] W. C. Hurty, ''Dynamic analysis of structural systems using component modes,'' AIAA J. **3**, 678–685 (1965).

[14] L. E. Suarez and M. P. Singh, ''Modal synthesis method for general dynamic systems,'' Trans. ASCE, J. Eng. Mech. **118**, 1488–1503 (1992).

[15] G. M. L. Gladwell, ''Branch mode analysis of vibrating systems,'' J. Sound Vib. **1**, 41–59 (1964).

[16] L. Cheng and R. Lapointe, ''Vibration Attenuation of panel structures by optimally shaped viscoelastic coating with added weight consideration,'' Thin-Walled Struct. **21**, 307–326 (1995).

[17] Y. C. Fung, *An Introduction to the Theory of Aeroelasticity* (Wiley, New York, 1955), Chap. 1, pp. 19–27.

[18] J. Neter and W. Wasserman, *Applied Linear Statistical Models* (Irwin, Homewood, IL, 1974).

[19] Y. C. Qu, L. Cheng, and D. Rancourt, ''Rotational compliance measurement of a flexible plane structure using an attached beam-like tip. Part II: Experimental study,'' Trans. ASME, J. Vib. Acoust. **119**, 603–608 (1997).